Nonstereogenic α-aminoisobutyryl-glycyl dipeptidyl unit nucleates type I′ β-turn in linear peptides in aqueous solution

ARTICLE *in* BIOPOLYMERS · JANUARY 2007

Impact Factor: 2.39 · DOI: 10.1002/bip.20738 · Source: PubMed

6 AUTHORS, INCLUDING:

Larry R. Masterson
Hamline University
32 PUBLICATIONS **625** CITATIONS
SEE PROFILE

Fernando Porcelli
Tuscia University
40 PUBLICATIONS **849** CITATIONS
SEE PROFILE

Robert P. Hammer
Ra Pharmaceuticals, Inc.
113 PUBLICATIONS **2,612** CITATIONS
SEE PROFILE

Gianluigi Veglia
University of Minnesota Twin Cities
173 PUBLICATIONS **3,811** CITATIONS
SEE PROFILE

Nonstereogenic α-Aminoisobutyryl-Glycyl Dipeptidyl Unit Nucleates Type I′ β-Turn in Linear Peptides in Aqueous Solution

Larry R. Masterson[1], Marcus A. Etienne[2], Fernando Porcelli[3], George Barany[1], Robert P. Hammer[2], Gianluigi Veglia[1,4]

[1] *Department of Chemistry, University of Minnesota, 207 Pleasant Street SE, Minneapolis, MN 55455*

[2] *Department of Chemistry, Louisiana State University, 232 Choppin Hall, Baton Rouge, LA 70803*

[3] *Department of Environmental Sciences, University of Tuscia, Viterbo, Italy*

[4] *Department of Biochemistry, Molecular Biology, and Biophysics, University of Minnesota, 4-104 Nils Hasselmo Hall, 312 Church St, Minneapolis, MN 55455*

Received 30 January 2007; revised 27 March 2007; accepted 28 March 2007
Published online 10 April 2007 in Wiley InterScience (www.interscience.wiley.com). DOI 10.1002/bip.20738

ABSTRACT:

The use of α,α-disubstituted amino acids represents a valuable strategy to exercise conformational control in peptides. Incorporation of the nonstereogenic α-aminoisobutyryl-glycyl (Aib-Gly) dipeptidyl sequence into i + 1 and i + 2 positions of an acyclic peptide sequence, originally designed and investigated by Gellman and coworkers, [H-Arg-Tyr-Val-Glu-Val-Yyy-Xxx-Orn-Lys-Ile-Leu-Gln-NH_2] nucleates a stable [2:4] left-handed type I′ β-turn in water. NMR spectra show that this newly designed β-hairpin does not aggregate in water up to a concentration of ∼ 1 mM, and that its backbone conformation is superimposable on corresponding hairpins containing the DPro-Gly (literature) and Aib-DAla (this work) sequences. The Aib-Gly turn-inducer sequence eliminates complications because of cis–trans isomerization of Zzz-Pro bonds, and constitutes an attractive alternative to the proteogenic Asn-Gly and nonproteogenic DPro-Gly motifs previously suggested as turn-inducer sequences. These design principles could be exploited to prepare water-soluble β-hairpin peptides with robust structures and novel function. © 2007 Wiley Periodicals, Inc. Biopolymers (Pept Sci) 88: 746–753, 2007.

Keywords: β-turn; $C^{\alpha,\alpha}$-disubstituted amino acids; α-aminoisobutyric acid; β-hairpin; conformational analysis; protein folding; NMR

This article was originally published online as an accepted preprint. The "Published Online" date corresponds to the preprint version. You can request a copy of the preprint by emailing the Biopolymers editorial office at biopolymers@wiley.com

Correspondence to: Gianluigi Veglia; e-mail: veglia@chem.umn.edu
Contract grant sponsor: ACS (Petroleum Research Fund)
Contract grant number: 42027-AC4
Contract grant sponsor: NIH
Contract grant numbers: AG17983, GM51628, GM64742
Contract grant sponsor: NSF
Contract grant number: BIR-961477
Contract grant sponsor: University of Minnesota Medical School

INTRODUCTION

Understanding of protein folding and progress in *de novo* protein design have advanced greatly over the past two decades,[1–3] as epitomized by the design of helix-based functional proteins.[4] The importance of *β*-sheet structures as motifs in protein native states,[5] as common determinants of protein–protein interactions,[6] and as central to certain misfolding pathways, including

amyloidogenesis,[7,8] is countered by more limited success in deciphering the principles behind their folding and harnessing those for design and function. A major reason why β-sheet models are more difficult to study relates to their ready tendency to self-associate in aqueous solution. Studies where secondary structure was determined in crystalline lattices or detected by biophysical techniques in the presence of organic solvents are of uncertain biological relevance.

More recently, several research groups have reported the synthesis and characterization of short peptide sequences (12–25 amino acid residues) that fold into stable, monomeric β-hairpins in aqueous solution.[9–12] Such sequences are often based on core regions excised from naturally occurring proteins such as ubiquitin, BPTI, GB1, tendamistad, etc.[9,11,13-15] or they incorporate designed turns with proteogenic[16–18] as well as nonproteogenic (e.g., D-stereochemistry, α,α-disubstituted, etc.) amino acids,[19–22] and/or they incorporate designed cross-strand side-chain interactions.[11,21,23-27] A key aspect towards designing stable, nonaggregating β-sheets, pioneered by Gellman and coworkers, is how exactly to engineer residues in the $i + 1$ and $i + 2$ turn positions so as to confer the proper handedness of a four-residue β-turn.[19,28,29] Thus, the so-called "mirror image" type I′ (e.g., proteogenic Asn-Gly)[16,17,30] and type II′ (e.g., nonproteogenic DPro-Gly)[9,10] turns are compatible with the natural right-handed twist of the sheets.[9,10]

The present article reports the first detailed structural characterization in aqueous solution of an hairpin peptide containing the nonstereogenic α-aminoisobutyryl-glycyl (Aib-Gly) dipeptidyl sequence as a turn inducer. The Aib-Gly turn design rationale rests on ample literature precedent, often supported by crystallographic structures, that the dialkylated Aib residue restricts ϕ/ψ space to helical or turn-like conformations.[31–34] Establishing Aib as a practical element of β-turns in hairpins opens the door for design based on other turn-favoring α,α-disubstituted residues. For example, functionalized α-tetrasubstituted amino acids like 4-aminopiperidine carboxylic acid[35] may serve as a convenient handle for incorporation of additional recognition elements in the design of hairpin peptides involved in molecular recognition.[36]

As a template, we use an acyclic peptide sequence designed and investigated previously by Gellman and coworkers,[19,28,37] i.e., H-Arg-Tyr-Val-Glu-Val-**Yyy-Xxx**-Orn-Lys-Ile-Leu-Gln-NH_2. The original peptide, with Yyy = DPro and Xxx = Gly, is referred to as **Ω^{D}PG**, whereas our nonstereogenic structure, with Yyy = Aib and Xxx = Gly, is referred to as **ΩBG**. Two stereogenic controls, **ΩB^{D}A**, with Yyy = Aib and Xxx = DAla, and **ΩAG**, Yyy = LAla and Xxx = Gly, have also been studied. We demonstrate here by solution NMR that **ΩBG** as well as **ΩB^{D}A** each feature a type I′ β-turn, and that the overall folds are closely comparable with that reported in the literature[19] for **Ω^{D}PG**.

MATERIALS AND METHODS

Materials

Protected Fmoc-amino acid derivatives, as well as Fmoc-PAL-PEG-PS supports (initial loading 0.18–0.22 mmol/g) for peptide synthesis, were mainly from Applied Biosystems (Framingham, MA). Additional protected derivatives were from NovaBiochem (Darmstadt, Germany). Piperidine (pip), 1,8-diazabicyclo[5.4.0]undec-7-ene (DBU), and triisopropylsilane (TIPS) were from Aldrich (Milwaukee, WI). Trifluoroacetic acid (TFA), *N,N*-dimethylformamide (DMF), and *N,N*-diisopropylethylamine (DIEA) were from Fisher (Pittsburgh, PA), and phenol crystals were from Mallinckrodt (St. Louis, MI). 1-Hydroxybenzotriazole (HOBt), *N*-[(1*H*-benzotriazol-1-yl)(dimethylamino)methylene]-*N*-methylmethanaminium tetrafluoroborate (TBTU), *N*-[(dimethylamino)-1*H*-1,2,3-triazolo[4,5-*b*]pyridin-1-yl-methylene]-*N*-methylmethanaminium hexafluorophosphate *N*-oxide (HATU), and 7-azabenzotriazolyoxytris(pyrrolidino)phosphonium hexafluorophosphate (PyAOP) were from Applied Biosystems.

Peptide Synthesis, Purification, and Characterization

Peptides were synthesized by standard solid-phase Fmoc chemistry carried out in the continuous-flow mode on a Pioneer Peptide Synthesizer, starting with Fmoc-PAL-PEG-PS (Peptide Amide Linker)-resin (0.2 mmol scale, 0.18 mmol/g loading). Side-chain protecting groups were Pbf for Arg, Trt for Gln, tBu for Glu, and Boc for Lys and Orn. Washings between reactions were carried out with DMF. Fmoc group deprotection was achieved using pip-DBU-DMF (1:1:48) for 5 min. Unless indicated otherwise, molar equivalents are given with respect to resin-bound amine. Couplings were carried out, after a minimal preactivation times, for 1 h with 4 equiv. each of Fmoc-amino acid, TBTU, and HOBt (final concentration of each = 0.25*M*), dissolved in 0.5*M* DIEA in DMF, except where noted. Alternatively, difficult couplings were carried out for 1 h with 4 equiv. each of Fmoc-amino acid and HATU (final concentration of each = 0.25*M*) dissolved in 0.5*M* DIEA in DMF, or with 4 equiv. each of Fmoc-amino acid and PyAOP (final concentration of each = 0.25*M*) dissolved in 0.5*M* DIEA in DMF for 1 h at 50°C; for these latter heated couplings, the normal resin column was fitted with a 100-mm OMNI column jacket (6331, OMNI Fit), which was connected to a Lauda Model WK230 circulating waterbath. Once chain assembly was complete, peptides were cleaved from the solid support using Reagent B (88:5:5:2, TFA:phenol:water:TIPS).[38] Approximately 10 mL of cleavage solution was added to 500 mg of resin and allowed to shake for 2 h. The cleaved peptide-resin was filtered, and then rinsed with 2 mL of TFA which was added to the original cleavage filtrate. The combined solutions were partially concentrated by rotary evaporation at 35°C to reduce the amount of TFA to approximately half the original volume. This partially concentrated solution was added dropwise into a 10-fold excess of cold ether, and the peptide was allowed to precipitate at −27°C for 24 h. The suspension of peptide in ether was centrifuged at 4 × 10,000 rpm, and the result-

ant pellet was washed (three times) and then dried for 4 h under vacuum. HPLC was performed on one of three systems: (1) Waters 600E multisolvent delivery system with a Model 486 tunable detector controlled by Empower Software, detection at 220 nm; (2) Waters 625 pump with a Model 996 diode array detector controlled by Millennium software, detection from 200 to 400 nm; (3) Waters Deltaprep system with detection at 220 nm. Three different columns were used for analysis and purification of peptides: (Column A) analytical HPLC was performed using a Vydac analytical C-18 (5 μm, 300 Å) reversed-phase column (218TP54, 4.6 × 250 mm) at 1 mL/min; (Column B) analytical and semipreparative chromatography was performed on a δ-Pak C_4 (15 μm, 100 Å) reversed-phase column (8 × 100 mm), at 1 mL/min; (Column C) preparative HPLC was performed on a Waters δ-Pak C_4 (15 μm, 100 Å) reversed-phase cartridge (25 × 10 mm) in a radial compression module at 15 mL/min. Linear gradients of 0.1% aqueous TFA in H_2O (v/v) (Buffer A) and 0.1% TFA in CH_3CN (v/v) (Buffer B) were used in all HPLC. Fractions from semipreparative or preparative HPLC were analyzed by matrix-assisted laser desorption ionization-time of flight (MALDI-TOF) on a Bruker Proflex III instrument with XMASS software.

Amino acid analysis was performed on a Dionex AAA-Direct system composed of a GS50 Gradient Pump, an AS50 Autosampler, and an ED50 Electrochemical Detector. Peptides were hydrolyzed in 1 mL Pierce vacuum hydrolysis tubes using 6*N* HCl for 24 h at 110°C. Hydrolyzates were separated on a microbore anion exchange column, AminoPac PA10 (2 × 250 mm) with a ternary gradient of deionized water, 0.25*M* sodium hydroxide, and 1.0*M* sodium acetate. Quantitation was performed with Pierce Amino Acid Standard H, diluted to produce a four-level calibration curve of 18 amino acids from 50 to 200 pmol, and including norleucine as an internal standard, using PeakNet software.

All peptides required for this work were obtained in excellent HPLC homogeneities (> 99% by analytical HPLC) after preparative HPLC purification, with good agreement between calculated and observed MALDI-MS data, and with peptide content estimated by amino acid analysis in the 60–89% range. The most straightforward syntheses, featuring TBTU/HOBt/DIEA couplings for all residues, were of **ΩAG** (calcd for MH^+ 1389.72, found 1389.45; initial crude purity 85%) and **Ω^{D}PG** (calcd for MH^+ 1415.65, found 1415.71; initial crude purity 98%). However, an initial synthesis of **ΩBG**, using HATU/DIEA double couplings specifically for Aib and the following amino acid (Val5), was found to be only 22% pure (t_R of desired 32.3 min on Column B with gradient of 10–70% B over 60 min), with a major byproduct identified as a deletion of Val5 located on the N-terminal side of Aib6. To rectify this problem, the **ΩBG** peptide was synthesized a second time using PyAOP/DIEA double couplings at 50°C for Aib6 and Val5 (calcd for MH^+ 1403.75, found 1403.16; crude purity 93%; t_R 14.8 min). Finally, the same modified protocol using heat for the difficult couplings was applied effectively to synthesize **ΩB^{D}A** (calcd for MH^+ 1416.77, found 1416.77; crude purity 79%; t_R 12.6 min).

CD Spectroscopy

All measurements were carried out using an Aviv Circular Dichroism Spectrometer Model 62DS with Igor plotting software. The CD instrument was calibrated using a 1.0 mg/mL solution of camphorsulfonic acid. Samples were prepared from a dilution of stock peptide sample (~1 m*M*) and NaOAc buffer (100 m*M*, pH = 3.8) in water to acquire a working solution of 50–500 μM peptide concentration in NaOAc (1 m*M* pH = 3.8). CD spectra were the average of three scans made at 1.00-nm intervals acquired from 260 to 190 nm (UV absorbance range). The spectrum of NaOAc buffer (1×) was used as the background subtraction in all experiments.

NMR Spectroscopy

The two peptides **ΩBG** and **ΩB^{D}A** were dissolved in 200 m*M* sodium acetate buffer, containing 10% D_2O at pH 3.8 (uncorrected for isotopic effect). NMR spectra of **ΩBG** and **ΩB^{D}A** (1 m*M*) were recorded at 278.1 K on a 600-MHz Varian Inova four-channel NMR spectrometer operating at 600.13 MHz. 1D ^{1}H spectra acquired in a range of temperatures from 278.1 to 306.1 K were used to calculate temperature coefficients for the amide protons. Resonance assignments were based on 2D-[^{1}H-^{1}H]-TOCSY (spin-lock field strength of 5.5 kHz and spin-lock times of 50 and 75 ms) and 2D-[^{1}H-^{1}H]-ROESY (spin-lock field strength of 5.5 kHz and spin-lock times of 100, 200, 350, and 400 ms) experiments using a spectral width of 5.5 kHz in both dimensions. The water signal was suppressed using the WATERGATE pulse sequence.[39] To measure $^3J_{HN\text{-}HA}$ couplings, a 2D-[^{1}H-^{1}H] DQF-COSY experiment was acquired with 2048 complex points in the direct dimension and 128 complex points in the indirect dimension using 40 scans for each increment. 2D-[^{1}H-^{1}H]-ROESY and TOCSY experiments were acquired with 2194 complex points in the direct dimension and 128 complex points in the indirect dimension using 64 scans for each increment. NMR spectra were processed using NMRPipe,[40] and the data points in both dimensions were weighted with a sine-squared function, and then zero filled to double the number of points prior to Fourier transformation. Linear prediction was used in the indirect dimensions to improve spectral resolution. Baseline corrections were applied to both dimensions using a fifth order polynomial.

NMR Structure Determination

Intra- and inter-residue dipolar contacts for the peptides were identified using a 2D-[^{1}H-^{1}H]-ROESYspectrum (400 ms mixing time), and the structures were calculated using X-PLOR-NIH using the classical simulated annealing protocol.[41] A total of 88 ROEs consisting of 86 inter- and two intraresidue ROEs were used for **ΩBG**, whereas a total of 153 ROEs consisting of 49 inter- and 104 intraresidue ROEs were used for **ΩB^{D}A**. Peak intensities from the ROESY spectra at 400 ms mixing time were converted into distances using the following classifications[19,37]: strong (1.8–2.8 Å), medium (1.8–3.5 Å), weak (1.8–5.0 Å), and very-weak (1.8–6.0 Å). Starting from extended conformations for both peptides, the calculations were carried out using an initial temperature (T_i) of 1000 K, 12,000 high temperature steps, and 6000 cooling steps with a step size of 5 fs. A total of 100 conformers were generated for both **ΩBG** and **ΩB^{D}A**. The 100 conformers were further refined by introducing van der Waals radii and Lennard-Jones potentials gradually, using a T_i of 300 K, 100,000 cooling steps, with a step size of 1 fs. Seventy-five structures were then selected for the final analysis with the following selection criteria: no ROE violations >0.5 Å, no bond violations >0.05 Å, and no dihedral violations >5°. Subsequently, 20 lowest energy conformers were selected with violations <0.3 Å, and the

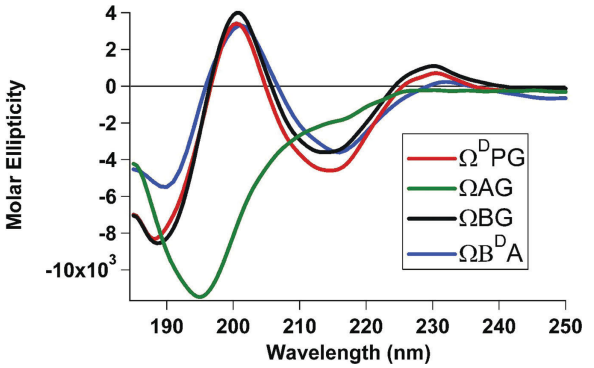

FIGURE 1 CD spectrum of Ω^{D}PG (DPro-Gly) overlayed with Ω*YX* (B = Aib) turn variants. Scans were taken at 50 μM peptide concentration in 1 m*M* NaOAc buffer; pH 3.8 at 25°C. (Molar ellipticity—[θ] units: deg cm^2 dmol^{-1}).

final structures were visualized using the MOLMOL software package.[42]

RESULTS AND DISCUSSION

The initial structural analysis of the peptides was performed by circular dichroism (CD) spectroscopy in aqueous buffer solution (see Figure 1). Two bands, a negative at ~217 nm (n–π^* transitions) and a positive at 197 nm (π–π^* transitions) are the dichroic signatures for β-sheet secondary structures.[43,44] Additionally, turns have their own dichroic profiles, which have been elucidated through the use of model cyclic and linear peptides. Typically, type I and type II′ turns have dichroic profiles similar to those of α-helices, whereas type II and type I′ have β-sheet-like profiles.[44] Thus, interpretation of hairpin CD spectra will need to account of both sheet and turn dichroic components. The CD of **Ω^{D}PG** shows a two-band dichroic profile with a maximum ~200 nm ($\Omega = 4000$) and a minimum at 215 nm ($\Omega = -4000$) that suggests significant sheet and turn structure in agreement with Gellman's studies (Figure 1, red line).[23] The CD spectrum of **ΩAG** (Figure 1, green line) shows a strong negative band centered at 195 nm ($\Omega = -12{,}000$), which is typical for a random coil peptide. The Aib-containing peptides **ΩBG** and **ΩB^{D}A** show CD profiles (Figure 1, black and blue lines, respectively) that almost overlay with that of **Ω^{D}PG**, indicating that they form similar structures in aqueous solution. Tenfold increase in the concentration of **Ω^{D}PG**, **ΩBG**, and **ΩB^{D}A** showed no change in the Ω values, suggesting that the absence of aggregation in these peptides (data not shown). Temperature-dependent CD of **Ω^{D}PG**, **ΩBG**, and **ΩB^{D}A** from 5 to 55°C showed only small changes in CD signatures and failed to give isodichroic points that would be suggestive of two-step unfolding (data not shown).

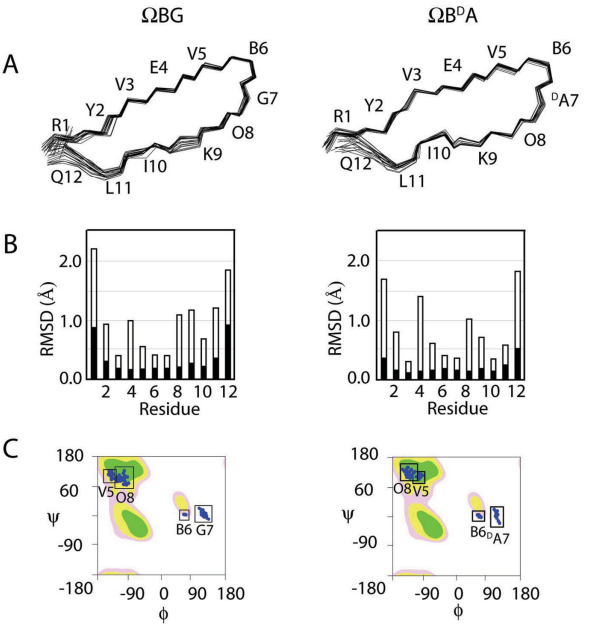

FIGURE 2 (A) Backbone superposition of the 20 lowest energy structures for the **ΩBG** and **ΩB^{D}A** peptides. (B) Histograms of the RMSD versus residue number for both peptide backbone (black) and side chains (white). (C) Ramachandran plots representing the distribution of ϕ and ψ angles for residues involved in the canonical type I′ β-turn.

To understand the structural details of these newly designed Aib-turn containing peptides at the atomic level, we carried out NMR spectroscopy in aqueous solutions, focusing on **ΩBG**, **ΩB^{D}A**, and **Ω^{D}PG**, which gave dichroic signatures of folded peptides.

Table I Comparison of Back-Calculated ^3J-Coupling Constants From the Average Structure ($^3J_{model}$) With Those Obtained From Measurements of DQF-COSY Data on ΩBG ($^3J_{measured}$) to Check the Veracity of the Calculated Structure

Residue	ϕ[a]	$^3J_{model}$	$^3J_{measured}$	$\Delta^3J_{model-measured}$
Y2	−125.9	9.62	8.41	0.57
V3	−122.3	9.69	9.60	0.06
E4	−143.9	8.52	7.00	1.02
V5	−136.9	9.10	9.60	−1.00
B6	64.0	6.87	N/A	N/A
G7	111.9	3.47	N/A[b]	N/A
O8	−110.5	9.51	9.63	−0.83
K9	−74.6	6.04	7.80	−1.90
I10	−130.7	9.46	9.60	−0.47
L11	−68.0	5.19	7.19	−2.71

Coupling constants along the backbone of the average solution structure were at most ~2 Hz of the experimentally measured constants, with the exception of L11 which precedes the *C*-terminal residue.

[a] ϕ angle given in degrees.

[b] Both diastereotopic Gly Hα's were found to have *J*-coupling values larger than 12 Hz.

Table II ϕ and ψ Angles for Each Residue In the Bundle of NMR Structures Corresponding to Ω^{D}PG, ΩBG, and ΩB^{D}A

	Torsional Angles (deg)					
	Ω^{D}PG		ΩBG		ΩB^{D}A	
Residue	ϕ	ψ	ϕ	ψ	ϕ	ψ
Arg(1)	—	139.3 ± 94.9	—	153.3 ± 15.7	—	146.0 ± 15.3
Tyr(2)	−106.6 ± 29.3	140.6 ± 25.2	−125.9 ± 9.7	146.4 ± 8.4	−121.5 ± 3.7	122.2 ± 14.1
Val(3)	−105.8 ± 17.4	135.0 ± 18.9	−122.3 ± 10.3	153.9 ± 3.1	−111.9 ± 9.0	127.3 ± 2.7
Glu(4)	−104.9 ± 16.8	117.2 ± 9.3	−143.9 ± 6.4	135.6 ± 6.2	94.6 ± 5.1	112.4 ± 5.3
Val(5)	−138.9 ± 8.9	142.9 ± 0.0	−136.9 ± 4.7	124.1 ± 4.1	−124.3 ± 7.2	129.5 ± 4.6
Xxx(6)	38.0 ± 5.3	−126.0 ± 4.3	64.0 ± 1.1	2.6 ± 0.3	63.8 ± 1.2	1.1 ± 0.3
Yyy(7)	60.5 ± 5.4	55.1 ± 4.5	111.9 ± 2.2	6.9 ± 5.8	114.3 ± 4.3	9.4 ± 9.6
Orn(8)	−151.3 ± 3.9	120.6 ± 21.1	−110.5 ± 9.6	112.1 ± 13.1	−125.9 ± 9.3	114.2 ± 4.1
Lys(9)	−96.9 ± 9.9	129.5 ± 5.6	−74.6 ± 6.0	141.1 ± 14.4	−84.4 ± 3.9	125.2 ± 5.8
Ile(10)	−123.2 ± 18.3	134.1 ± 24.6	−130.7 ± 13.7	120.3 ± 13.3	90.6 ± 2.1	122.3 ± 3.0
Leu(11)	95.5 ± 12.8	121.5 ± 19.1	−68.0 ± 8.9	133.3 ± 5.8	86.4 ± 3.9	114.4 ± 10.5
Gln(12)	−135.6 ± 25.8	—	−145.1 ± 74.0	—	145.9 ± 9.6	—

Calculations were performed using the software MOLMOL.

Under NMR conditions, **ΩBG** and **ΩB^{D}A** showed an absence of aggregation over a concentration range of 100 μM–1 mM as monitored by the chemical shifts and the lineshapes of the one-dimensional ^{1}H NMR spectra. Figure 2 summarizes results from NMR analysis and structural calculations determined on the **ΩBG** and **ΩB^{D}A** peptides. Figure 2A shows the backbone superposition of the final 20 ensembles with the lowest energy structures. To determine the convergence of obtained structures, only residues 2–11 were considered, whereas both unstructured termini were excluded from the final analysis. The peptide backbone is well defined, with an average root-mean-square deviation (RMSD) of 0.34 ± 0.16 Å (**ΩBG**) and 0.33 ± 0.12 Å (**ΩB^{D}A**) for superposition of backbone atoms (Figure 2B, black bars). The average RMSD for heavy atoms of the amino acid residue side-chains was 1.5 ± 0.3 Å (**ΩBG**) and 1.14 ± 0.32 Å (**ΩB^{D}A**) (Figure 2B, white bars). To validate the backbone structure for **ΩBG** determined using ROE constraints, we back-calculated $^{3}J_{\mathrm{HN\text{-}H\alpha}}$ coupling constants for residues 2–11. We found that the ^{3}J-coupling for those residues are within ∼2 Hz of the

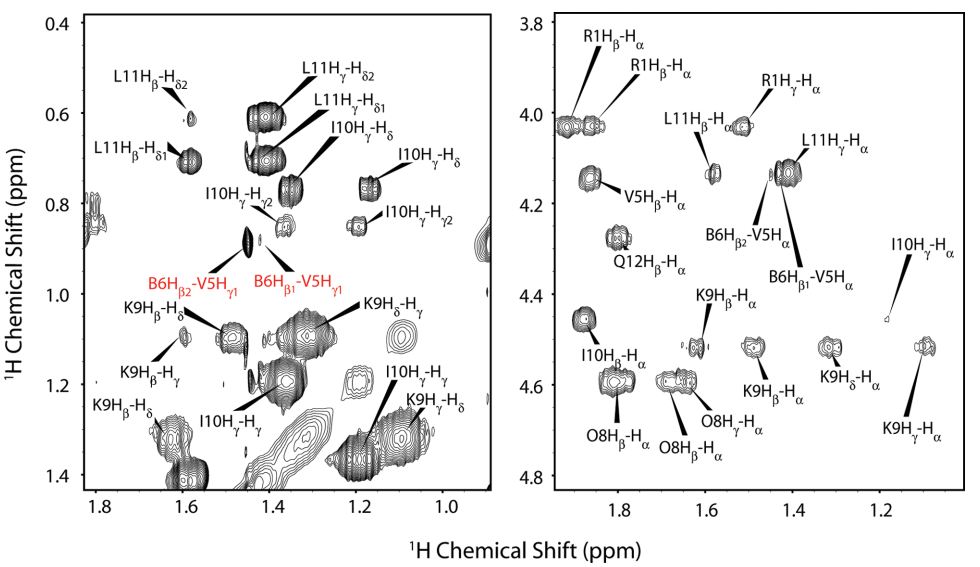

FIGURE 3 Representative ROESY spectra acquired with a mixing time of 300 ms on a 600-MHz spectrometer showing the resolved Aib methyl side chains (red) that generate dipolar contacts in distinct environments. The proR methyl group of Aib corresponds to protons labeled as HB2, while those for the proL methyl group correspond to HB1.

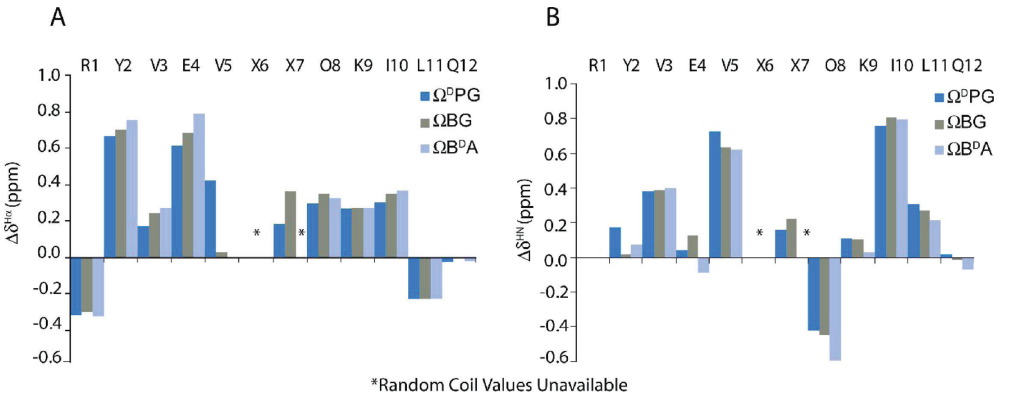

FIGURE 4 (A) Comparison of H_α and (B) H_N chemical shift indices of **Ω^{D}PG**, **ΩBG**, and **ΩB^{D}A**.

values determined experimentally by the analysis of DQF-COSY data (Table I).

Both the Aib-Gly and the Aib-DAla sequences induce a left-handed type I′ β-turn (Figure 2C; Table II). As with the literature-reported structure of **Ω^{D}PG**,[19] numerous informative nonsequential ROEs in these peptides derive from interstrand side-chain–side-chain interactions. In particular, a dense network of dipolar contacts was detected between Tyr2 on one strand and Leu11 and Lys9 on the opposite strand; these three residues constitute a tight cluster below the plane of the β-sheet. The diagonal pairing between Tyr2 and Lys9 is considered diagnostic of a right-handed twist in the strands. Furthermore, two sets of signature pairwise cross-strand NH–NH interactions are present in both of these peptides: Val3 and Val5 with Ile10 and Orn8, respectively.

The residues that constitute the loop are clustered into the expected regions of the Ramachandran plot (Figure 2C). Val5 and Orn8 are located in the extended (sheet-like) region of the ϕ/ψ plot, as is expected for the i and $i+3$ residues of a type-I′ β-turn.[1,19] For both **ΩBG** and **ΩB^{D}A**, numerous dipolar contacts occur with residues at the $i+1$ (Aib6) and $i+2$ (Gly7 or ^{D}Ala7) positions of the four-residue turn, which stabilize it in a left-handed conformation, as has been precedented.[10,34,45] Finally, differential peak intensities between the Aib6 methyl groups with the neighboring Val5 H_γ and H_α are also indicative of a conformational preference at the turn region (see Figure 3).

To identify the differences in conformations and register of the **Ω^{D}PG**, **ΩB^{D}A**, and **ΩBG** peptides, we plotted the chemical shift indices, i.e., the deviations of H_α (Figures 4A) and H_N (Figure 4B) chemical shifts, relative to random coil standards.[46] The close, general agreement of the index values suggests that the three peptides have essentially superimposable folds. The preponderance of downfield Ha shifts for residues 2–4 and 8–10, an the HN downfield shifts of residues 2–4 and 8–11 are suggestive of β-strand formation.[47] The upfield H_α shifts of Leu11 and Gln12 in these peptides is likely because of their proximity to the aromatic ring of Tyr2, as has been precedented.[48]

An overlay of the backbone for the three peptides is reported in Figure 5. Notably, the folding of the peptides is not affected and the three conformations are virtually identical. In fact, the RMSD among the minimized average structures is ∼0.4 Å, a value that is comparable with the distribution of the conformers within each structural ensemble. Moreover, all three peptides adopt a [2:4] type I′ β-turn with a left-handed twist (see Table II). The only differences that can be inferred from these structures are the lengths of the backbone hydrogen bonds (Figure 6). The structure of **Ω^{D}PG** shows longer hydrogen bonds, whereas the other two peptides (**ΩB^{D}A** and **ΩBG**) show more uniform lengths along the peptide backbone. This apparent discrepancy could be

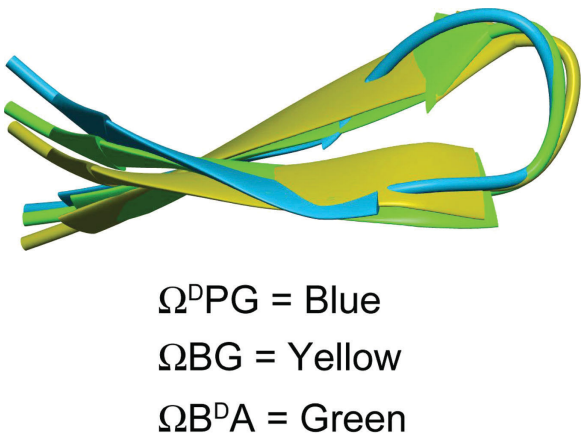

FIGURE 5 Superposition of the **Ω^{D}PG**, **ΩBG**, and **ΩB^{D}A** backbone traces. The average structures were calculated from 20 lowest energy conformers. The RMSD of the three average structures is ∼0.4 Å.

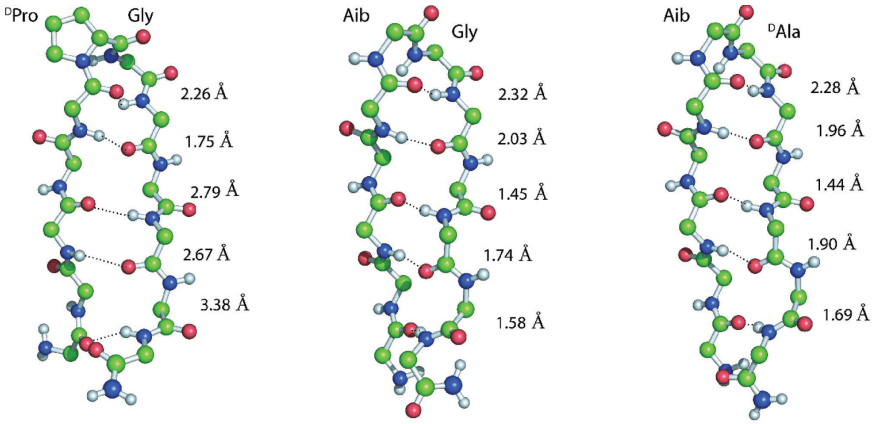

FIGURE 6 Comparison of the backbone hydrogen bond networks for **Ω^{D}PG**, **ΩBG**, and **ΩB^{D}A**, respectively.

explained by the different protocols used for the structural refinement calculations.

Further evidence of the structural similarity of **Ω^{D}PG** and **ΩBG** came from side-by-side NMR determinations of temperature gradient coefficients ($\Delta\delta/K$).[49] Linear plots were obtained for all inter-residue amide protons. The corresponding slopes in each peptide agreed within ±5% (Figure 7), with the exception of the Tyr2, which is in close proximity to the N-terminus. In both peptides, the Orn8 H_N showed a $\Delta\delta/K$ value outside of the envelope for other residues by a factor of ~3, suggesting that this residue may be involved in a hydrogen bond that stabilizes the β-hairpin structure.

Autonomously formed β-sheet peptides are ideal models to study principles of protein folding and design. We have shown here that when using templates with favorable cross-strand interactions, the achiral Aib-Gly sequence acts as an effective left-handed type I′ β-turn inducer with the resultant β-hairpin assuming a native-like right-handed twist. This is the same fold reported in the literature with the stereogenic DPro-Gly sequence, and found here with the stereogenic Aib-DAla sequence. The nature and stereochemistry of residues used at the $i + 1$ and $i + 2$ positions, while all other residues are the same, can be absolutely critical. It has been shown that folded structure is abolished by inversion of chirality at the $i + 1$ position (LPro replacing DPro; conclusion based on NMR evidence)[19] or even by removal at the $i + 1$ position of a pro-R methyl (LAla replacing Aib; Figure 1, green line). Moreover, adding a pro-*S*-methyl at the $i + 2$ position (i.e., creation of an achiral Aib-Aib dipeptidyl sequence) results in a random coil peptide. Additionally the Aib-Xxx turn inducing sequence circumvents the cis–trans isomerization of Zzz-Pro bonds[50] that often complicates structural characterization.[51,52]

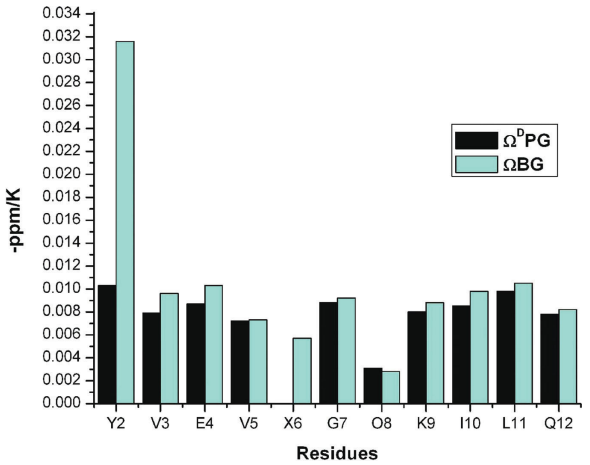

FIGURE 7 Temperature coefficients of the amide protons for **ΩBG** and **Ω^{D}PG** obtained over a range of 5–28°C in 3°C increments.

Overall, we have shown here that when working with a template predisposed to β-hairpin formation, engineering the achiral Aib-Gly sequence in place of the commonly used stereogenic DPro-Gly results in equivalent folding. Thus, conformational ensembles of β-hairpins generated with either Aib-Gly or DPro-Gly have comparable resolution, and the temperature coefficients of the two peptides are similar. The use of α-tetrasubstituted amino acids at the $i + 1$ position of type-I′ β-turns may be generalizable for use in peptide and protein design and in the development of ligands for biomolecular recognition, for which turn geometry and functionality are often key.[53]

CONCLUSION

In conclusion, we have found that stereogenicity is not a prerequisite for chiral turn induction, and that use of Aib-Gly provides a straightforward alternative to the more commonly used stereogenic Pro-Xxx turn sequences. We propose that the achiral Aib-Gly sequence can be exploited to prepare

water-soluble β-hairpin peptides with robust structures and novel functions.

We thank Professor Samuel Gellman for sharing the atomic coordinates of the Ω^{D}**PG** peptide, Catherine Thomas and Martha Juban for assistance in peptide synthesis, Dr. Tracy McCarley and Dr. Michelle Beeson for mass spectrometric analyses, and Professor Tim Keiderling for many helpful discussions.

REFERENCES

1. DeGrado, W. F.; Summa, C. M.; Pavone, V.; Nastri, F.; Lombardi, A. Annu Rev Biochem 1999, 68, 779–819.
2. Baltzer, L.; Nilsson, H.; Nilsson, J. Chem Rev 2001, 101, 3153–3163.
3. Magliery, T. J.; Regan, L. Eur J Biochem 2004, 271, 1595–1608.
4. DeGrado, W. F.; Gratkowski, H.; Lear, J. D. Protein Sci 2003, 12, 647–665.
5. Richardson, J. S.; Richardson, D. C. Proc Natl Acad Sci USA 2002, 99, 2754–2759.
6. Maitra, S.; Nowick, J. S. The Amide Linkage: Structural Significance in Chemistry, Biochemistry, and Materials Science, Chapter 15; Wiley: New York, 2000; pp 495-518.
7. Dobson, C. M. Nature 2003, 426, 884–890.
8. Cohen, F. E.; Kelly, J. W. Nature 2003, 426, 905–909.
9. Gellman, S. H. Curr Opin Chem Biol 1998, 2, 717–725.
10. Venkatraman, J.; Shankaramma, S. C.; Balaram, P. Chem Rev 2001, 101, 3131–3152.
11. Searle, M. S.; Ciani, B. Curr Opin Struct Biol 2004, 14, 458–464.
12. Hughes, R. M.; Waters, M. L. Curr Opin Struct Biol 2006, 16, 514–524.
13. Blanco, F. J.; Jimenez, M. A.; Herranz, J.; Rico, M.; Santoro, J.; Nieto, J. L. J Am Chem Soc 1993, 115, 5887–5888.
14. Carulla, N.; Woodward, C.; Barany, G. Biochemistry 2000, 39, 7927–7937.
15. Olsen, K. A.; Fesinmeyer, R. M.; Stewart, J. M.; Andersen, N. H. Proc Natl Acad Sci USA 2005, 102, 15483–15487.
16. Cochran, A. G.; Tong, R. T.; Starovasnik, M. A.; Park, E. J.; McDowell, R. S.; Theaker, J. E.; Skelton, N. J. J Am Chem Soc 2001, 123, 625–632.
17. Butterfield, S. M.; Waters, M. L. J Am Chem Soc 2003, 125, 9580–9581.
18. Pastor, M. T.; Gimenez-Giner, A.; Perez-Paya, E. ChemBioChem 2005, 6, 1753–1756.
19. Syud, F. A.; Stanger, H. E.; Gellman, S. H. J Am Chem Soc 2001, 123, 8667–8677.
20. Descours, A.; Moehle, K.; Renard, A.; Robinson, J. A. ChemBioChem 2002, 3, 318–323.
21. Espinosa, J. F.; Syud, F. A.; Gellman, S. H. Biopolymers 2005, 80, 303–311.
22. Setnicka, V.; Huang, R.; Thomas, C. L.; Etienne, M. A.; Kubelka, J.; Hammer, R. P.; Keiderling, T. A. J Am Chem Soc 2005, 127, 4992–4993.
23. Syud, F. A.; Stanger, H. E.; Mortell, H. S.; Espinosa, J. F.; Fisk, J. D.; Fry, C. G.; Gellman, S. H. J Mol Biol 2003, 326, 553–568.
24. Galzitskaya, O. V. Mol Biol 2002, 36, 607–612.
25. Blandl, T.; Cochran, A. G.; Skelton, N. J Protein Sci 2003, 12, 237–247.
26. Jimenez, M. A.; Barrachi-Saccilotto, A. C.; Valdivia, E.; Maqueda, M.; Rico, M. J Pept Sci 2005, 11, 29–36.
27. Bofill, R.; Simpson, E. R.; Platt, G. W.; Crespo, M. D.; Searle, M. S. J Mol Biol 2005, 349, 205–221.
28. Syud, F. A.; Espinosa, J. F.; Gellman, S. H. J Am Chem Soc 1999, 121, 11577–11578.
29. Espinosa, J. F.; Syud, F. A.; Gellman, S. H. Protein Sci 2002, 11, 1492–1505.
30. McElroy, A. B.; Clegg, S. P.; Deal, M. J.; Ewan, G. B.; Hagan, R. M.; Ireland, S. J.; Jordan, C. C.; Porter, B.; Ross, B. C.; Ward, P.; Whittington, A. R. J Med Chem 1992, 35, 2582–2591.
31. Awasthi, S. K.; Shankaramma, S. C.; Raghothama, S.; Balaram, P. Biopolymers 2001, 58, 465–476.
32. Aravinda, S.; Shamala, N.; Rajkishore, R.; Gopi, H. N.; Balaram, P. Angew Chem Int Ed Engl 2002, 41, 3863–3865.
33. Balaram, P. J Pept Res 1999, 54, 195–199.
34. Toniolo, C.; Crisma, M.; Formaggio, F.; Peggion, C. Biopolymers 2001, 60, 396–419.
35. Wysong, C. L.; Yokum, T. S.; Morales, G. A.; Gundry, R. L.; McLaughlin, M. L.; Hammer, R. P. J Org Chem 1996, 61, 7650–7651.
36. Athanassiou, Z.; Patora, K.; Dias, R. L.; Moehle, K.; Robinson, J. A.; Varani, G. Biochemistry 2007, 46, 741–751.
37. Wuthrich, K. NMR of Proteins and Nucleic Aids; John Wiley & Sons, 1986, Chapters 7–10.
38. Sole, N. A.; Barany, G. J Org Chem 1992, 57, 5399–5403.
39. Piotto, M.; Saudek, V.; Sklenar, V. J. J Biomol NMR 1992, 2, 661–665.
40. Delaglio, F.; Grzesiek, S.; Vuister, G. W.; Zhu, G.; Pfeifer, J.; Bax, A. J Biomol NMR 1995, 6, 277–293.
41. Schwieters, C. D.; Kuszewski, J. J.; Tjandra, N.; Clore, G. M. J Magn Reson 2003, 160, 65–73.
42. Koradi, R.; Billeter, M.; Wuthrich, K. J Mol Graphics 1996, 14, 51–55.
43. Sreerama, N.; Woody, R. W. Methods Enzymol 2004, 383, 318–351.
44. Greenfield, N. J. In Numerical Computer Methods, Part D: Analysis of Circular Dichroism Data, Vol. 383, 2004; pp 282-317.
45. Gunasekaran, K.; Ramakrishnan, C.; Balaram, P. Protein Eng 1997, 10, 1131–1141.
46. Merutka, G.; Dyson, H. J.; Wright, P. E. J Biomol NMR 1995, 5, 14–24.
47. Wishart, D. S.; Sykes, B. D.; Richards, F. M. J Mol Biol 1991, 222, 311–333.
48. Stanger, H. E.; Syud, F. A.; Espinosa, J. F.; Giriat, I.; Muir, T.; Gellman, S. H. Proc Natl Acad Sci USA 2001, 98, 12015–12020.
49. Andersen, N. H.; Neidigh, J. W.; Harris, S. M.; Lee, G. M.; Liu, Z. H.; Tong, H. J Am Chem Soc 1997, 119, 8547–8561.
50. Taylor, C. M.; Hardre, R.; Edwards, P. J. J Org Chem 2005, 70, 1306–1315.
51. Bruns, K.; Fossen, T.; Wray, V.; Henklein, P.; Tessmer, U.; Schubert, U. J Biol Chem 2003, 278, 43188–43201.
52. Shi, T. S.; Spain, S. M.; Rabenstein, D. L. J Am Chem Soc 2004, 126, 790–796.
53. Tyndall, J. D. A.; Pfeiffer, B.; Abbenante, G.; Fairlie, D. P. Chem Rev 2005, 105, 793–826.